

BIOLOGICALLY RELEVANT METAL COORDINATION COMPOUNDS: Mo^{VI}O₂ AND NICKEL(II) COMPLEXES WITH TRIDENTATE AROMATIC SCHIFF BASES

R. HAHN, W. A. HERRMANN,* G. R. J. ARTUS and M. KLEINE

Anorganisch-chemisches Institut, Technische Universität München,
 Lichtenbergstrasse 4, D-85747 Garching, Germany

(Received 12 December 1994; accepted 23 March 1995)

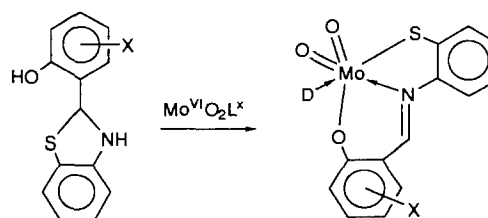
Abstract—The synthesis and characterization of two monomeric tridentate Schiff base complexes, Ni^{II}(*o*-O-C₆H₄-C=N-C₆H₄-*o*-S)(4-Bu¹-C₅H₄N) (**1**) and Mo^{VI}O₂(2-O-C₁₀H₆-C=N-C₆H₄-*o*-S)(CH₃-SO-CH₃) (**2**), is presented. The structure of both compounds has been determined by X-ray crystallography. Two terminal oxo groups *cis* to each other strongly influence the distorted octahedral geometry of the molybdenum complex **2**. Additionally, the tridentate dibasic Schiff base ligand coordinated to the dioxomolybdenum core exhibits an unusually large dihedral angle along the C=N bond of 40°. By way of contrast, the nickel complex **1** exhibits a nearly regular square planar coordination geometry in which the dihedral angle in the coordinated tridentate Schiff base ligand is only 1.3°. Different influences of tridentate dibasic Schiff base ligands on the geometry and solution chemistry of nickel(II) and Mo^{VI}O₂ complexes are discussed. The value of these ligands for the synthesis of model compounds of metalloenzymes is evaluated. The thermal decomposition (TG/MS) of the dimeric derivative of **1** is discussed.

For our comparative study we chose two metal centres with slightly different ionic radii ([Mo^{VI}O₂]²⁺, *r* = 59 pm and [Ni^{II}]²⁺, *r* = 55 pm)¹ and with relevance to enzymatic redox activity. Oxomolybdenum cores are known to play an essential role in the active site of molybdopterin-containing enzymes such as sulphur oxidase and xanthine oxidase.² Nickel is part of the active centre in enzymes involved in the metabolism of methane and urea in many organisms.³ In both biological systems a mixed SNO coordination sphere of the metal centre is assumed.

The properties of complexes containing tridentate dibasic Schiff base ligands shown in Fig. 1 are markedly dependent on the nature of the ligand donor atoms, the degree of delocalization in the π -system of the ligand and the substituent on the phenyl rings. These factors appear to be the main determinants of the electrochemical oxidation or

reduction potentials⁴ of the resulting complexes. The electrochemical parameters represent an important criterion in designing suitable model compounds for metal-containing redox enzymes. However, spectroscopic properties (IR, UV-vis etc.) vary within a small range.

Up to now Schiff base ligands were considered as quasi-planar ligands. The angle between the planes defined by the two aromatic systems generally var-



L¹H₂: X = H
 L²H₂: X = 3,4 Benzo-

Fig. 1. Synthesis of dioxomolybdenum(VI) complexes with dibasic Schiff base ligands.

* Author to whom correspondence should be addressed.

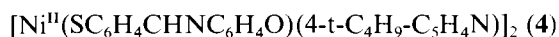
ies between 0 and 20°. Therefore, this feature of the complexes has not been considered as an important factor contributing to their physical parameters.

We present here the synthesis and characterization of a dioxomolybdenum Schiff base complex exhibiting a substantial deviation from planarity of the tridentate ligand. An additional tool to influence the physical parameters of these complexes is demonstrated. Furthermore, a detailed analysis of the solution and oligomerization behaviour of a nickel(II) core chelated by the tridentate ligand **L**¹ will be discussed. The behaviour of nickel(II) complexes with tridentate dibasic Schiff base ligands has been examined by Crabtree and co-workers.⁵ They found and characterized a variety of oligomeric compounds that seemed to exist in a solution equilibrium. Catalytic activity of some of these complexes for silane alcoholysis was observed.⁵

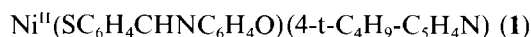
Our analysis will provide the background to discuss the utility of complexes containing tridentate Schiff base ligands for the design of bioinorganic model compounds.

EXPERIMENTAL

All manipulations were performed under argon using standard Schlenk techniques. All solvents were deaerated, dried and distilled before use. Reagents were AR grade or above and the starting materials MoO₂(acac)₂,⁶ *N*-salicylidene-(2-mercaptoaniline) (**L**¹H₂)⁷ and MoO₂(SC₆H₄CHNC₆H₄O) (**3**)⁸ were prepared according to previously reported syntheses. *N*-2-Hydroxy-1-naphthylidene-(2-mercaptoaniline) (**L**²H₂) and the corresponding dioxomolybdenum complex (**2**) were synthesized by the same procedure as **L**¹H₂ and **3**. Crystallization of **2** was carried out as described for **1**.



A solution of **L**¹H₂ (2.68 g) in ethanol (10 cm³) was added slowly to a solution of Ni(acac)₂ (3.0 g; Aldrich) in ethanol (20 cm³) and the mixture refluxed for 1 h. The brown precipitate formed was collected and washed with ethanol (2 × 50 cm³), diethyl ether (50 cm³) and pentane (50 cm³). A suspension of the product in ethanol (50 cm³) was then heated with one equivalent of 4-tert-butylpyridine until the solid dissolved completely. Addition of diethyl ether (100 cm³) precipitated a dark brown microcrystalline powder (4.03 g; 82%). Found: C, 61.9; H, 5.4; N, 6.5; S, 7.8; Ni, 13.9%. Calc. for C₂₂H₂₂N₂OSNi: C, 62.7; H, 5.3; N, 6.7; S, 7.6; Ni, 13.9%. Mass spectrometry (chemical ionization): M⁻ *m/z* 570; M⁺ *m/z* 135.



Dissolving compound **4** in dimethylsulphoxide (DMSO) and slow crystallization by vapour diffusion of water to the solution gave dark red crystals suitable for X-ray analysis. ¹H NMR (DMSO, ppm vs. TMS): δ 8.90 (s, 2H, —CH=N—); 8.83 (b, 4H, Bu¹-C₅H₄N); 7.88 (d, 2H); 7.70 (d, 2H); 7.56 (b, Bu¹-C₅H₄N); 7.30 (t, 2H); 7.24 (d, 2H); 7.01 (t, 2H); 6.93 (t, 2H); 6.78 (d, 2H); 6.67 (t, 2H); 1.30 [s, 18H, C(CH₃)₃]. ¹³C NMR (DMSO, ppm vs. TMS): δ 164.03 (—CH=N—); 157.17; 151.57; 150.24; 142.53; 134.73; 134.57; 127.34; 126.77; 122.21; 121.54; 120.53; 120.32; 116.47; 115.38; 50.34 [C(CH₃)₃]; 35.03 [C(CH₃)₃].

Crystal structure determination

X-ray structure determination of **1** and **2** (values for **2** are given in brackets). Final lattice parameters were obtained by least-squares refinement of 25 reflections (**1**: 40.3° < 2θ < 49.4°; **2**: 40.3 < 2θ < 48.6°; λ = 70.930 pm, Mo-K_α1). The space groups were identified from the systematic absences: **1**, orthorhombic, space group *Pbcn* (I.T. No. 60), *a* = 1787.3(3), *b* = 908.0(1), *c* = 2703.0(4) pm, *V* = 4386.5(1) × 10⁶ pm³, ρ_{calc} = 1.39 g cm⁻³, *Z* = 8; **2**, monoclinic, space group *P2₁/c* (I.T. No. 14), *a* = 823.9(1), *b* = 1305.2(2), *c* = 2198.5(3) pm, β = 100.16(1), *V* = 2327.1(5) 10⁶ pm³, ρ_{calc} = 1.64 g cm⁻³.

A deep red crystal of **1** (size: 0.41 × 0.51 × 0.38 mm) and a red needle of **2** (size: 1.03 × 0.18 × 0.21 mm) were mounted in glass capillaries on an Enraf-Nonius CAD4 diffractometer with Kappa geometry. Data were collected at -50°C in the range 2° < 2θ < 50° with graphite-monochromated Mo-K_α (λ = 71.073 pm) radiation using the ω-scan mode. All 4339 (6866) data were corrected for Lorentz and polarization terms using the SDP System.⁹ Both structures were solved by the Patterson method (SHELXS-86).¹⁰ All atoms were located from subsequent least-squares refinements and difference Fourier syntheses using the program CRYSTALS.¹¹ All non-hydrogen atoms were refined anisotropically; the disordered solvent molecule DMSO in **1** was partially refined isotropically. All hydrogen atoms were refined with isotropic displacement parameters, the hydrogen positions in the free solvent molecules were calculated in ideal geometry and were partially refined. Final refinement using 3239 (3716) unique reflections [**1**: *I*/σ(*I*) > 2.0; **2**: *I*/σ(*I*) > 1.0] converged at *R* = 0.036 (0.037), *R*_w = 0.037 (0.033). A final difference Fourier map was featureless. All calculations were

performed on a Micro VAX 3100 and on a DEC Station 5000/25.

Crystal data collection and refinement parameters of **1** and **2** are listed in Tables 1 and 2, respectively.

Thermogravimetry

The thermal decomposition of **4** was studied by thermogravimetry coupled with mass spectrometry (TG/MS). The measurements were performed using a Perkin–Elmer TGA 7 and a Balzers QMG 420 mass spectrometer coupled by means of a capillary system heated to 280°C. A sample (1.923 mg) was subject to a temperature program with a heating rate of 10 K min⁻¹ between 50 and 400°C in a dynamic helium atmosphere.

RESULTS AND DISCUSSION

Metal cores bearing ideally four coordination sites may form undercoordinated complexes with tridentate ligands. The coordination sphere is then completed by oligomerization or by addition of a monodentate ligand (solvent or others) (Fig. 2).

In some cases steric hindrance may inhibit such a reaction.¹²

In the absence of monodentate molecules, tridentate dibasic Schiff bases induce oligomeric structures of dioxomolybdenum(VI) compounds.¹³ The metal centres are connected through bridging oxygen atoms. Due to the lack of terminal oxo groups the oligomerization behaviour of the corresponding nickel complexes depends on the donor atoms of the chelating ligand. Crabtree and co-workers⁵ stated that oligomeric complexes bridged by thiolates or phenolates are formed in solution, and monomerization can be achieved by adding a strongly coordinating donating compound like DMSO or pyridine. The same procedure is used for the monomerization of the dioxomolybdenum(VI) analogues. A parallel behaviour in solution may therefore be assumed. However, the following paragraph will show by way of comparison that these reactions are much more complicated for the nickel(II) system than for the O₂Mo^{VI} complexes.

The reaction of L¹H₂ with Ni(acac)₂ in refluxing ethanol results in the polymeric Ni_x(L¹)_x. This compound can easily be solubilized by adding one equivalent 4-tert-butylpyridine per nickel atom. The

Table 1. X-ray crystallographic data for **1**

Formula	C ₂₂ H ₂₂ N ₂ NiOS · 1/2 C ₂ H ₆ OS
<i>M_r</i>	460.25
Crystal system	Orthorhombic
<i>a</i> (pm)	1787.3(3)
<i>b</i> (pm)	908.0(1)
<i>c</i> (pm)	2703.0(4)
<i>V</i> (10 ⁶ pm ³)	4386.5(9)
Space group	<i>Pbcn</i>
ρ_{calc} (g cm ⁻³)	1.39
Mo-K α (pm)	71.073
<i>Z</i>	8
<i>F</i> (000)	1928
μ (cm ⁻¹)	10.4
θ range (°)	1 < θ < 25
Scan mode	ω -scan
Temperature (°C)	-50 ± 3
Number of reflections measured	4339
Number of unique reflections	3536
Number of reflections used for refinement, $I/\sigma(I) > 2.0$	3239
Number of refined parameters	353
Parameters of Tukey and Prince ¹² weighting scheme	$p_1 = 1.26, p_2 = 0.0505, p_3 = 0.891,$ $p_4 = -0.123, p_5 = 0.152$
Maximum and minimum electron density in ΔF map (e Å ⁻³)	+0.63, -0.42
<i>R</i> ^a	0.036
<i>R_w</i> ^a	0.037

^a $R = \Sigma (|F_0| - |F_c|) / \Sigma |F_0|$, $R_w = [\Sigma w (|F_0| - |F_c|)^2 / \Sigma w F_0^2]^{1/2}$.

Table 2. X-ray crystallographic data for **2**

Formula	C ₂₁ H ₁₁ D ₂ MoNO ₅ S ₃ C ₁₇ H ₁₁ MoNO ₃ S · 2DMSO- <i>d</i> ₆
<i>M_r</i>	573.65
Crystal system	Monoclinic
<i>a</i> (pm)	823.9(1)
<i>b</i> (pm)	1305.2(2)
<i>c</i> (pm)	2198.5(3)
β (°)	100.16(1)
<i>V</i> (10 ⁶ pm ³)	2327.1(5)
Space group	<i>P</i> 2 ₁ / <i>c</i>
ρ_{calc} (g cm ⁻³)	1.64
Mo- <i>K</i> _α (pm)	71.073
<i>Z</i>	4
<i>F</i> (000)	1144
μ (cm ⁻¹)	8.4
θ range (°)	1 < θ < 25
Scan mode	ω -scan
Temperature (°C)	-50 ± 3
Number of reflections measured	6866
Number of unique reflections	3892
Number of reflections used for refinement, <i>I</i> / σ (<i>I</i>) > 1.0	3716
Number of refined parameters	349
Parameters of Tukey and Prince ¹² weighting scheme	<i>p</i> 1 = 2.20, <i>p</i> 2 = 2.95, <i>p</i> 3 = 2.43, <i>p</i> 4 = 1.12, <i>p</i> 5 = 0.526
Maximum and minimum electron density in ΔF map (e Å ⁻³)	+0.77, -1.22
<i>R</i> ^a	0.037
<i>R_w</i> ^a	0.033

$$^a R = \Sigma (||F_0| - |F_c||) / \Sigma |F_0|, R_w = [\Sigma w (|F_0| - |F_c|)^2 / \Sigma w F_0^2]^{1/2}.$$

isolated compound is identified as a dimeric complex containing two moles of 4-*tert*-butylpyridine. Data from mass spectrometric analysis (chemical ionization) are coherent with a dimeric structure of the type **4**, shown in Fig. 3. The most intense peak appears at *m/z* 570 for the dimeric pyridine-free complex. During cathodic scans 4-*tert*-butylpyridinium is detected. The elemental analysis of compound **4** corresponds to the proposed structure.

TG/MS exhibits an interesting decomposition pattern of the compound (Fig. 4) and confirms the dimeric structure of the complex. From 50 to 207°C one equivalent of 4-*tert*-butylpyridinium is evolved

in two hardly resolved steps (-8.72%, -7.14%, *m/z* 135). Up to 312°C another equivalent (-18.03%, *m/z* 135) is evolved. The following well-shaped step from 312 to 400°C represents fragmentation of the tridentate ligand (*m/z* 93: C₆H₅O⁺; 91: PhNH⁺; 227: L¹, -44.56%). The residue (21.57%) may be NiS (theor.: 21.58%).

Dissolution of compound **4** in DMSO produces a brown solution which quickly changes to a dark orange-red colour. Dark red crystals suitable for X-ray diffraction study were obtained after slow diffusion of water into the saturated solution. Spectrometric, elemental analysis and X-ray diffraction

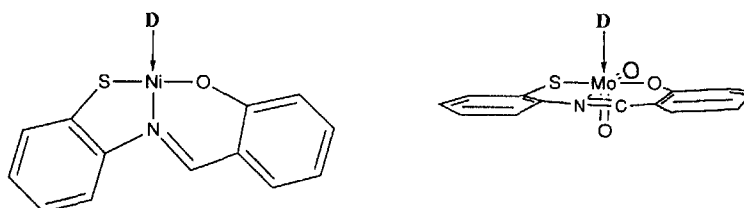


Fig. 2. Open coordination site (D) on O₂Mo^{VI} and nickel(II) complexes with tridentate Schiff bases.

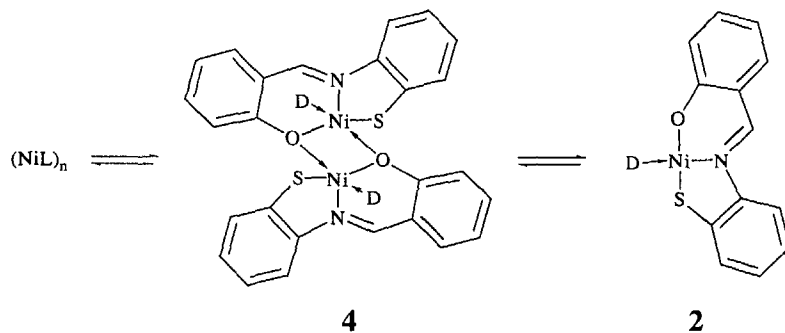


Fig. 3. Oligomerization equilibria of $Ni_x(L^1)_x D_y$ in solution.

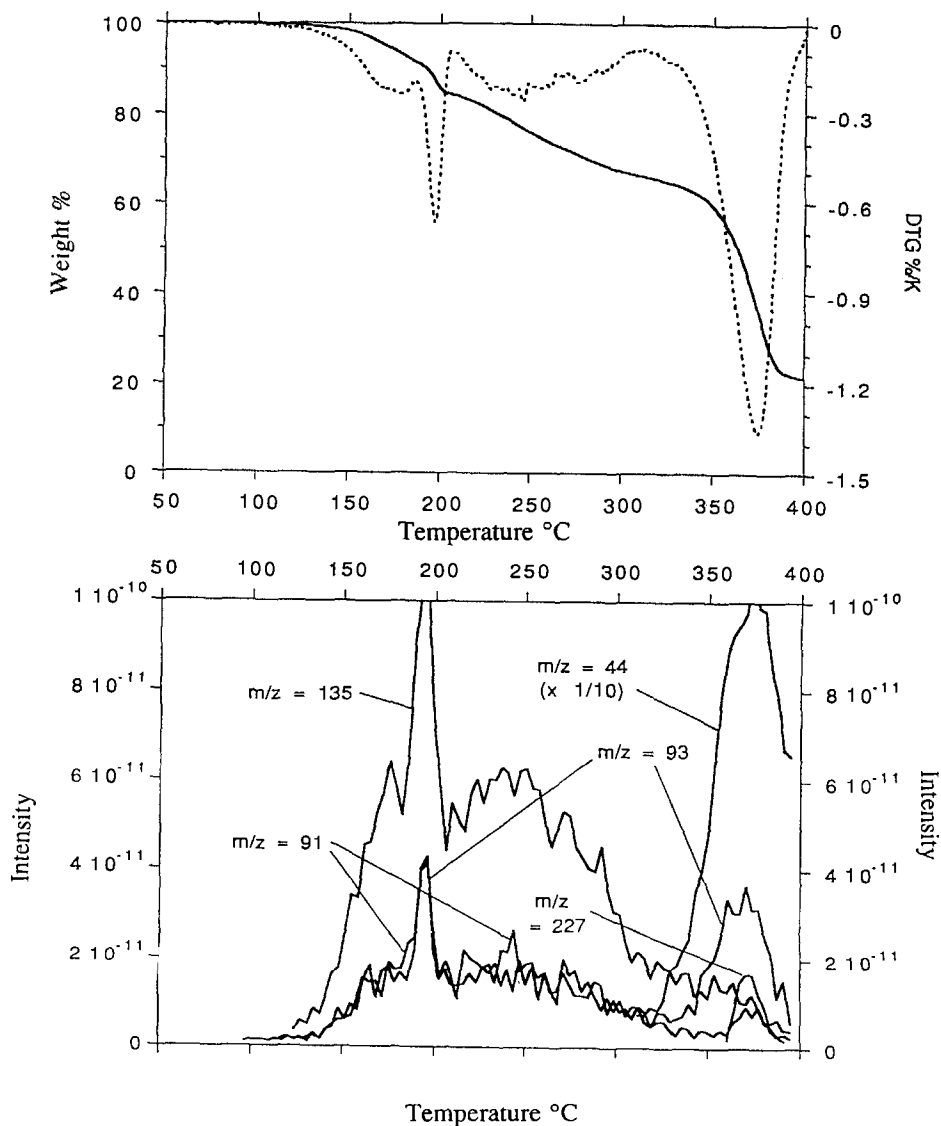


Fig. 4. Thermal decomposition of **4** studied by thermogravimetry (TG/MS).

data confirmed the monomeric structure of compound **1** (Fig. 5). The former dimeric structure of the *tert*-butylpyridine adduct is split by adding DMSO. However, the strongly coordinating pyridine ligand remains on the nickel(II) centre.

It becomes clear from this analysis that the oligomeric character of dibasic tridentate Schiff base nickel complexes is directed by the polarity of the solvent and the presence of strongly coordinating bases such as pyridine. The equilibria in solution are therefore much more intricate than previously assumed (Fig. 3).

Oligomerization of these compounds is mainly due to the ability of four-coordinate nickel(II) compounds to increase their coordination number. The degree of oligomerization can be directed by judicious choice of solvent, a feature that has not been observed for the analogous O_2Mo^{VI} systems. Thus, the influence of the solvent is of considerable importance for the study of such compounds, in comparison to natural systems where monomeric systems are encountered more frequently.

The low spin nickel(II) complex **1**, shown in Fig. 5, exhibits a quasi-square planar geometry with an almost ideal planarity of the ligand system. No effects are observed that would induce a distorted tetrahedral geometry. The angle between the two planes defined by the phenyl rings is only 1.3° . Interatomic distances are within the normal ranges for nickel(II) coordination complexes.

While the chemical properties of **1** offer insights into the solution chemistry of these complexes, the corresponding O_2Mo^{VI} (**2** and **3**) complexes reveal some interesting structural features. Comparison of the structural data of **1** and $L_1Mo^{VI}O_2$ (**3**) demonstrates that this ligand type may bend considerably in the C=N bridge between the phenyl rings (Table 3) in the presence of *trans*-standing

oxo groups, as shown in compound **3**.⁸ The metal-to-Schiff-base-nitrogen distance is strongly increased from 188.3 to 231.2 pm, and the angle between the planes of the two substituted phenyl rings increases from near planarity up to 19° .

On the other hand, the O_2Mo^{VI} system induces a much stronger distortion in the naphthyl-derived ligand, L^2H_2 , which is not a result of an increased *trans* effect. In complex **2** (Fig. 6) an angle of 40° between the two aromatic systems is measured. Steric interaction of protons may be excluded. We therefore propose electronic reasons for the strongly increased dihedral angle.

This assumption is supported by spectroscopic and electrochemical measurements. The stretching frequencies of the O_2Mo^{VI} core are slightly changed from **3** to **2**. In particular, the asymmetric stretching vibration in **2** (891 cm^{-1}) appears 30 wavenumbers higher than in compound **3**, which indicates a strengthening of the Mo=O bond. However, the symmetrical vibration slightly decreases by 13 wavenumbers (930 cm^{-1} , **3**; 917 cm^{-1} , **2**). Also, the reduction potential decreases by 60 mV from **3** to **2**.

Ligand L^2 obviously exhibits greater flexibility. Participation of the C=N π -bond in the total π -system in L^2 is much smaller than in L^1 . Therefore, the distortion energy in the bonds adjacent to the C=N group seems to be decreased, which is reflected by the dihedral angles in **2** in comparison to **3**. The stress put on the ligand by the *trans* influence of the oxo groups can more easily be answered by ligand L^2 than by L^1 .

Table 3 illustrates the increased deviation from ideal octahedral geometry around the molybdenum centres in **3** and **2**, and some parameters defining the arrangement of the ligands compared to some structural features of the nickel complex **1**.

This structural study demonstrates the possibility of influencing the geometry of $Mo^{VI}O_2$ complexes using Schiff bases bearing, on one side of the ligand, an expanded π -orbital system. The electrochemical parameters are shifted. This point is particularly important in the design of new model compounds for metals in the active sites of redox enzymes. We enhanced the flexibility of the Schiff base ligand by increasing the aromatic system. As a consequence, the MoO_2 system shifts to an electrochemically more stable state. Therefore, we conclude that the higher the geometric rigidity or the delocalization of the π -system in the complex, the easier the O_2Mo^{VI} compound may be reduced.

CONCLUSION

Tridentate Schiff base ligand systems still offer new insights into the coordination chemistry of bio-

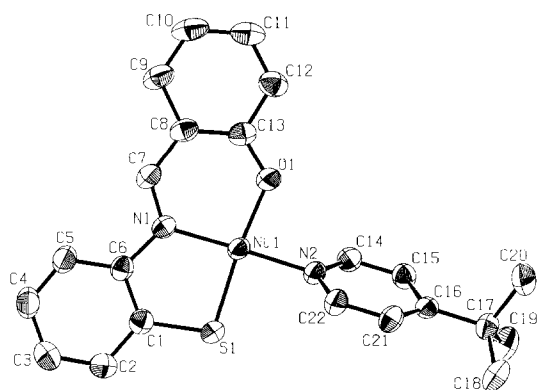


Fig. 5. Platon plot¹⁴ of **1**, with thermal ellipsoids drawn at the 50% probability level. Hydrogen atoms are omitted for clarity.

Table 3. Selection of angles and interatomic distances in mononuclear tridentate Schiff base complexes with Ni^{II} (1) and Mo^{VI}O₂ (2, 3) cores

Angle/distance ^a	1 M=Ni	3 M=Mo ^b	2 M=Mo
M—O ¹	—	170.3(1)	170.2(2)
M—O ²	—	170.1(2)	170.2(2)
M—O ^L	185.2(2)	194.9(1)	197.0(2)
M—N ^L	188.3(2)	231.2(2)	229.7(2)
M—S ^L	214.57(7)	241.0(0)	243.87(7)
N ^L —C(6)	143.1(3)	142.6(3)	142.2(3)
N ^L —C(7)	130.6(3)	128.7(3)	129.0(3)
S ^L —C	174.3(2)	175.6(2)	175.8(3)
O ^L —C	129.6(3)	133.9(2)	134.0(3)
C(7)—C(8)	141.8(4)	144.3(3)	143.8(3)
O ¹ —M—O ²	—	105.33(8) ^c	104.3(1) ^c
O ¹ —M—O(4)	—	166.68(7) ^c	167.65(8) ^c
O ² —M—N ^L	N(2)—Ni—N ^L 175.96(8) ^c	163.24(7) ^c	163.93(8) ^c
O ^L —M—S ^L	172.59(6) ^c	154.94(5) ^c	152.25(6) ^c
N ^L —M—S ^L	89.56(6) ^c	78.70(4) ^c	77.80(5) ^c
N ^L —M—O ^L	96.41(8) ^c	83.48(6) ^c	79.40(7) ^c
<(Ph ¹ —Ph ²)	1.3 ^c	18.5 ^c	40.2 ^c

^a N^L, S^L, O^L: donor atoms of the tridentate ligand; O¹: terminal oxo ligand *trans* to donor molecule DMSO; O²: terminal oxo ligand *trans* to ligand N^L atom.

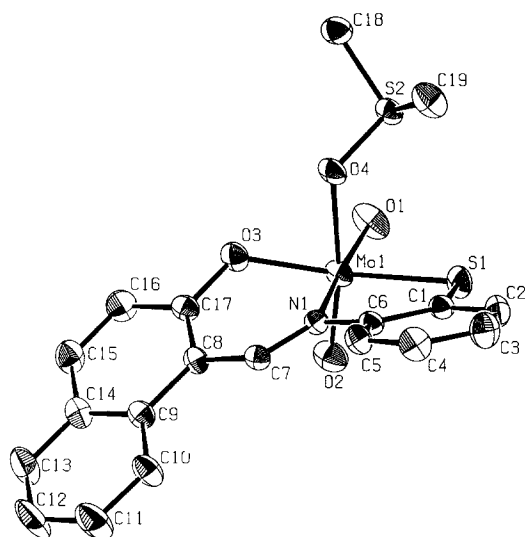


Fig. 6. Platon plot¹⁴ of 2, with thermal ellipsoids drawn at the 50% probability level. Hydrogen atoms are omitted for clarity.

logically relevant metal (oxo) ions such as [Ni^{II}]²⁺ and [O₂Mo^{VI}]²⁺. The present study reveals new perspectives for the design of model compounds for molybdopterin-containing enzymes using Schiff base ligands with an enlarged π -system. It is shown that ligand rigidity may be responsible for the shift of physical parameters of tridentate Schiff base O₂Mo^{VI} complexes, in addition to the above-mentioned parameters. Furthermore, comparative

investigations regarding the coordination geometry on [Ni^{II}]²⁺ and [O₂Mo^{VI}]²⁺ centres with tridentate dibasic Schiff bases are presented. Our investigation leads to the conclusion that, in contrast to the dioxomolybdenum(VI) systems, the complicated oligomerization behaviour of nickel(II) complexes in solution makes control of the solution chemistry difficult. Therefore, O₂Mo^{VI} systems of this type are more suitable as model compounds for natural metal centres than the corresponding nickel(II) complexes.

Acknowledgement—Financial support of this work by the Deutsche Forschungsgemeinschaft is gratefully acknowledged.

REFERENCES

1. R. D. Shannon, *Acta Cryst.* 1976, **A32**, 751.
2. J. H. Enemark and C. G. Young, *Adv. Inorg. Chem.* 1993, **40**, 1.
3. J. R. Lancaster Jr, (Ed.), *The Bioinorganic Chemistry of Nickel*. VCH, New York (1988); P. A. Lindahl, N. Kojima, R. P. Hausinger, J. A. Fox, B. K. Theo, C. T. Walsh and W. H. Orme-Johnson, *J. Am. Chem. Soc.* 1984, **106**, 3062; A. Chapman, R. Cammack, C. E. Hatchikian, J. McCracken and J. Peisach, *FEBS Lett.* 1988, **242**, 134; R. Cammack, *Adv. Inorg. Chem.* 1988, **32**, 297.
4. J. Topich and J. O. Bachert, *Inorg. Chem.* 1992, **31**, 511.

5. D. E. Barber, Z. Lu, T. Richardson and R. H. Crabtree, *Inorg. Chem.* 1992, **31**, 4709; Z. Lu, C. White, A. L. Rheingold and R. H. Crabtree, *Inorg. Chem.* 1993, **32**, 3991; Z. Lu, C. White, A. L. Rheingold and R. H. Crabtree, *Angew. Chem.* 1993, **105**, 121.
6. H. Gehrke Jr and J. Veal, *Inorg. Chim. Acta* 1969, **3**, 623.
7. W. E. Hill, N. Atabay, C. A. McAuliffe, F. P. McCullough and S. M. Razokki, *Inorg. Chim. Acta* 1979, **35**, 35.
8. J. Topich and J. T. Lyon III, *Polyhedron* 1984, **3**, 55; R. Hahn, U. Küsthardt and W. Scherer, *Inorg. Chim. Acta* 1993, **210**, 177.
9. B. A. Frenz, Enraf–Nonius “SDP”-Plus Structure Determination Package, Version 4.0. Enraf–Nonius, Delft, The Netherlands (1988).
10. G. M. Sheldrick, SHELXS-86. Universität Göttingen, Germany (1986).
11. D. J. Watkin, P. W. Betteridge and J. R. Carruthers, *CRYSTALS User Manual*. Oxford University Computing Laboratory, Oxford (1986).
12. J. M. Berg and R. H. Holm, *Inorg. Chem.* 1983, **22**, 1768; J. M. Berg and R. H. Holm, *J. Am. Chem. Soc.* 1984, **106**, 3035.
13. R. H. Holm, *Chem. Rev.* 1987, **87**, 1401; R. H. Holm, *Coord. Chem. Rev.* 1990, **100**, 183; R. H. Holm and J. P. Donahue, *Polyhedron* 1993, **12**, 571.
14. A. L. Spek, *Acta Cryst.* 1990, **A46/C34**.